ANSP

Comparison of the effects of graphene and nanoclay nanosheets on crystalline structure of polyvinylidene fluoride

Ali Akbar Yousefi[1]

[1] Energy Division, Iran Polymer and Petrochemical Institute, P.O. Box 14965/115, Tehran, Iran

ABSTRACT

An extensive review of the literature showed that both graphene and Cloisite 30B nanosheets are widely employed to modify the crystalline structure and piezoelectic properties of polyvinylidene fluoride (PVDF). Due to the similarity in the geometry of these nanoparticles a comparative study is reported to find the stems of difference in their effects on crystalline structure of PVDF. Scanning electron microscopy (SEM) of these composites showed that large and wide graphene particles are dispersed in PVDF matrix whereas their thickness is well below 100 nanometers. Meanwhile, a careful inspection of SEM micrographs of Cloisite 30B loaded composites revealed existence of smaller particles with almost the same particles thicknesses. Both techniques of Fourier transform infrared (FT-IR) spectroscopy and wide angle X-ray diffraction (WXRD) witnessed changes in the crystalline structure of PVDF. The overall finding was that Cloisite 30B improves the polar beta phase of PVDF crystals, whereas a revers effect was found in the presence of graphene nanosheets. These observations were accounted for by differences in surface geometry and surface free energy (surface tension and interfacial tension). Based on the data available for surface properties of these two nanosheets it was found that surface properties of Cloisite 30B is very close to those of PVDF, whereas the surface properties of graphene are far from those of PVDF. Also a lower interfacial tension was found to be active in PVDF-Cloisite 30B system compared to that operative in PVDF-graphene system. An intimate interface along with proper surface texture led to higher content of PVDF's beta crystals in case of Cloisite 30B nanocomposite.

Keywords

PVDF, Cloisite 30B, graphene, surface free energy, morphology

1. Introduction

Polyvinylidene fluoride (PVDF, chemical formula of $[CH_2CF_2]_n$) is a technically important polymer due to its almost unique physical properties. The chemical inertness and polar chemical structure of PVDF result in another share in technical importance and applications of PVDF. These make PVDF polymer of the choice in many insulation and membrane applications. Amongst the important physical properties on PVDF are its ferroelectric properties such as piezo- and pyroelectric properties which are profited in sensor applications [1]. These properties are a consequence of PVDF crystalline structure [2, 3]. The crystalline structure of PVDF is affected by many factors. Amongst these factors the role of processing conditions (stretching) [2], solvent [4] and additives [5, 6] are the most prominent ones. Stretching diversely affects polymer chains morphology and properties. For example it leads to:

* Corresponding Author Email: a.yousefi@ippi.ac.ir

-chains orientation, alpha (TGTG' conformations) to beta (all-trans conformation) crystal conversion, -machine direction (MD) mechanical properties enhancement and transverse direction (TD) mechanical properties reduction.

Stretching induces oriented beta crystals which are piezo and pyro-electrically active. However, stretching deteriorates the mechanical properties of the stretched films in machine transverse direction and also reduces the total crystal contents of the film. To put an end to this withdrawal of stretching many workers tried to use different physical modifiers to enhance the beta crystal content of PVDF parts avoiding reductions in mechanical properties [6, 7]. Nanotechnology and nano materials are also profited in PVDF–based piezo sensors [8]. Different workers tried to employ nanomaterials to facilitate preparation of PVDF piezo-devices through bypassing stretching the PVDF preforms [9, 10]. Among diverse categories of nano materials, nanoclays [8-10], carbon nanotubes [11, 12] and graphene nanosheets [13, 14] and mixture of nano-materials [6, 15, 16] were employed to transform PVDF crystals.

Nanomaterials are divided into different categories based on particles' geometry and composition. For example, clay and carbonaceous particles could be further divided into particles, fibers tubes and sheets (flakes). Two types of nano-sheets are extensively used to modify PVDF crystalline structure. These are nanoclay and graphene nano-sheets. Naoclay sheets were first used to reinforce polyamide 6 as timing belt cover by Toyota car making company in 1960's [17]. Since then the consumption of thermoplastic polymers showed a jumping leap compared to that of thermosets. However,

incorporation of nanoclay into PVDF was first reported in 2002 [8]. In this paper by Priya and Jog, Solef 1008 grade of PVDF with a polydispersity index (PDI=M_w/M_n) equal to 2.5 was melt-mixed with organically modified Cloisite 6A. In this paper mutual interactions of PVDF and Cloisite 6A were presented. It was reported that according to XRD patterns PVDF crystalline structure of PVDF underwent alpha to beta structure conversion. Meanwhile, the XRD patterns of nanoclay shifted towards lower 2theta and fades. They also reported an increases in melting temperature and crystallization rate. They found interesting results and continued this investigation later [17, 18]. An interesting finding is that in spite of non-polar tallow of organically modified clay, some improvements in the elasticity (E') were observed. Later Pramoda et al [19] also melt mixed PVDF and nanoclay and discovered that beta phase crystals of PVDF are formed in the presence of clay nanosheets. They also reported an increase in storage modulus of the nano-composite in a wide range of temperature. Pallathadka et al [20] confirmed formation of beta crystal in PVDF in the presence of nanoclay using solid state NMR.

Dillon et al [21] solution cast and co-precipitated PVDF nano-composite using two different organically modified clays. They found that in solution cast samples phase separation and intercalation took place depending on the type of organic tallow, whereas exfoliation was observed under any conditions. Yu et al [22] studied the effect different nanoclay contents on the crystalline structure of PVDF. They found that at clay contents below 0.4wt% both alpha and gamma crystals coexist. At clay contents higher than 1wt%, alpha

and beta crystals coexist. Patro et al [23] studied the effect of differently modified nanocalys on crystalline structure of PVDF by melt mixing in a mini twin-screw extruder. They reported that beta crystals are formed in the presence of clay particle and that the extent of clay dispersion depends on the organic modification loaded on clay. They also found that the clay acts as nucleating agent, the crystal melting points 10 to 13 degrees increased and lamella sizes were decreased.

Yu and Cebe [24] studied the effect of nanoclay on the crystalline structure and dielectric relaxation of PVDF. They reported that at high clay concentration there would be a prefered tendency towards fully beta crystal formation. Using dielectric relaxation spectroscopy (DRS) they introduced two relaxation rates that is α_a (glass transition process, polymer chain motions in the amorphous zones) and α_c (polymer chain motions in the crystals and fold surfaces). It was reported that both relaxation rates increase in the presence of clay particles. This was attributed to the segregation of polymer chains in the presence of clays. Another finding of this research was that the electrical conductivity showed a 4-fold increase for the composites as compared with that of neat PVDF.

Yousefi and Salarian [25] studied the effect of Cloisite 30B on the crystalline structure of PVDF. This research showed that incorporation of this grade of nanoclay in PVDF leads to 11-fold increase in beta crystal content of PVDF. To reconfirm the effect of nanocaly on the crystalline structure of PVDF a low percentage of polyamide 6 (PA6) was added to the nanocomposite. They found that due to higher tendency PA6 toward nanoclay the beta crystal content of PVDF reduced to its pure form. Another finding of this research also in the field of rheology of the nanocomposite was that the rheological properties of the nanocomposite are reduced in the presence of clay nanoparticles. This finding was consistent with other researches [24]. In a comparative study the effects of 0.5, 1 and 2wt% of CNT, nanoclay and crystalline cellulose on the crystalline structure of PVDF were studied [26]. It was reported that nanoclay follows crystalline cellulose with a small differences at higher concentration, whereas nanoclay behaves better at lower concentration. Recently, Roopa et al [27] spin coated thin film of PVDF/Cloisite 15A and observed about 83% of beta crystal conversion (500rpm for 35 min) and the film showed -18 to -25 pC/N at 110Hz and 0.25N. In 2019 a Brazilian research team [28] electrospun nanoclay and dodecylbenzene sulfonic acid—doped polypyrrole. In the next step this nanocomposite was used to modify PVDF by electrospinning and solution casting. Authors claimed that the beta crystals are prominent but no quantitative value was reported.

Graphene is one-atom-thick planar sheet of carbon atoms [29] with exceptional properties such as values of Young's modulus (1.1 terra Pascal), large theoretical specific surface area (2630 m^2/g) and superb thermal conductivity (almost 5000 W/m.s) [30]. Graphene particles are very similar to nanoclay particles as far as their geometry is considered. Ansari and Gialennis [31] reported using graphene oxide (GO) as a modifier for PVDF. They prepared their composites by solution casting and reported co-existence of alpha and beta crystals in PVDF without any quantification of crystals shares. Graphene oxide nanosheets were solution

mixed with PVDF using dimethyl formamide (DMF) as solvent by ElChaby et al [32]. Authors reported that purely beta crystals were formed only at 0.1wt% of GO nanosheets due to interactions between graphene oxide carbonyl group and -CF2 groups in PVDF. Below this concentration of GO nanosheets a mixture of alpha and beta crystals are formed. ElChaby et al in another work [33] incorporated graphene nanosheets into PVDF but no data was provided on the crystalline structure of PVDF. Ataur Rahman and Chaung [34] also solution blended GO and PVDF in DMF and reported formation of 100% beta crystals. The cast film was maintained at 70°C to evaporate the solvent and then hot pressed. Jang et al [35] incorporated up to 10wt% graphene and observed no beta crystals and proposed graphene as alpha phase promoting filler. Liu et al [36] used graphene oxide to solution cast films of nanocomposite and found that hot-pressing leads to lost of carbonyl groups on GO. This provokes beta to alpha crystal transformation.

Mohamadi et al [37] reported that graphene nanosheets at the presence of poly methyl methacrylate (PMMA) and DMF increase the content of polar crystals of PVDF. Huang et al [38] used different contents of reduced graphene oxide (rGO) in PVDF. They reported around 100% beta crystal for 0.1wt% rGO in PVDF. The d_{33} for this composition reported to be -39pC/N. Wang et al [39] reported that in the presence of graphene nanosheets the rate of polar crystals (gamma form) formation increases. An et al also confirmed formation of beta crystals in solution cast PVDF/GO films [40]. Other workers also confirmed formation of beta crystals in the presence of GO

[41-43]. Fortunato et al incorporated thermally expanded graphene oxide nano sheets into PVDF and observed a reduction in beta crystals of the nanocomposites. In an unexpected manner they reported an increase in d_{33} coefficient of piezoelectricity in case of nanocomposites [44].

According to the reviewed literature a comparative study is missing and it would be beneficiary in the field of PVDF nanocomposites. Therefore, in this paper the effects of melt-mixed Cloisite 30B and graphene nanosheets on the crystalline structure of PVDF were compared and the effectiveness of nanocaly was highlighted. A structural mechanism was proposed for this difference in crystalline structure.

2.Experimental

2.1.Materials

PVDF granules (Hylar460, Solvay Company, Belgium) were used as received. Graphene nanosheets from Asbury Carbons, USA and nanoclay (Cloisite 30B, BYK Additives & Instruments, Germany) were used as received without any further treatment or purification.

2.2.Methods

Nanoclay and graphene particles were melt-mixed with PVDF using a Haake internal mixer at 230°C at a rotor speed of 60rpm. The rate of modification was fixed at 0.5 and 1wt% of modification for both graphene and nanoclay.

The crystalline structure of hot-pressed film samples was studied by Fourier transformed infrared spectroscopy (FT-IR, Bruker Equinox 55) and X-ray diffraction (XRD, D5000, CuKα,

Siemens, Germany). The β-phase content of the FT-IR samples was calculated using Eq. 1. [4]

$$F(\beta) = \frac{A_\beta}{1.26A_\alpha + A_\beta} \qquad (1)$$

where F(β) is the relative fraction of β-phase, A_α and A_β are the absorbance of vibration band at 763 and 840 cm⁻¹, respectively. Scanning electron microscopy (SEM, Vega II, Czech Republic) was used to examine the morphology of the cross-section of the nanocomposites. The SEM specimens were broken under liquid nitrogen manually and gold coated prior to be scanned at an acceleration voltage of 20kV.

3.Results and discussion
3.1.Morphology

In Figures 1 and 2 graphene particles in PVDF matrix of 0.5 and 1wt% modified nanocomposites are presented, respectively. As clearly seen in these figures, the thickness of the graphene particles varies between 65 and 90 nanometers. It could be concluded that an increase in particles concentration from 0.5 to 1wt% causes more inter-particle interactions which in turn leads to a reduction in platelets thickness. It is observed that increase in particle concentration (reinforcing rate) results in a more effective viscous shearing and a finer dispersion. Consequently, the number of thinner particles is augmented. Compared with pure graphene nanosheets (Figure 3), it is concluded that particles are undergone multiple delaminations. As seen in Figures 1 and 2 an intimate adhesion of PVDF matrix is clear, meanwhile, long pull out of nanosheets are observed. These show that polymer chains are in close contact of graphene outer surface

but strong interactions are not active at the nanocomposite interface. It is not expected that these weak interaction could strongly affect PVDF crystalline structure.

In Figures 3 and 4 nanoclay particles of 0.5 and 1wt% modified nanocomposites are shown. In contrast to their graphene counterparts it is observed that the thickness of the nanoclay particles are approximately the same but the number of particles is increased with reinforcement concentration. Comparing with graphene nanocomposites, it can be concluded that interlayer attractive forces in graphene nanosheets are weaker than those active between nanoclay nanosheets. As seen, the width of nanocaly particles is smaller than those of graphene nanosheets, whereas the thickness of the clays is the same as those of graphene nanosheets. Inspection of these figures reveals that nanoclay sheets are of round edges, no particle break is observed and the length of particle pull out is very short. Accordingly, significant nanoclay-polymer interactions are expected. Based on these observations profound changes in PVDF crystalline structure are expected.
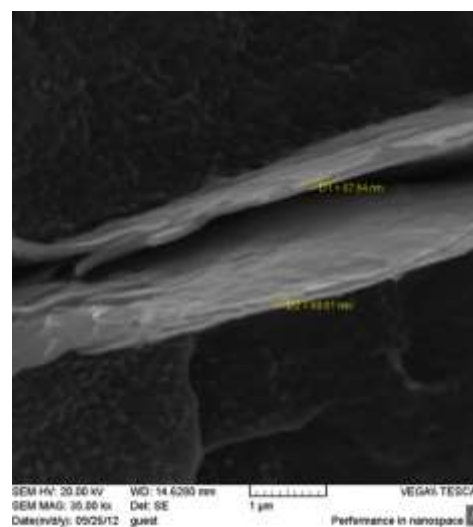
Figure 1: Scanning electron micrograph of 0.5% graphene in PVDF
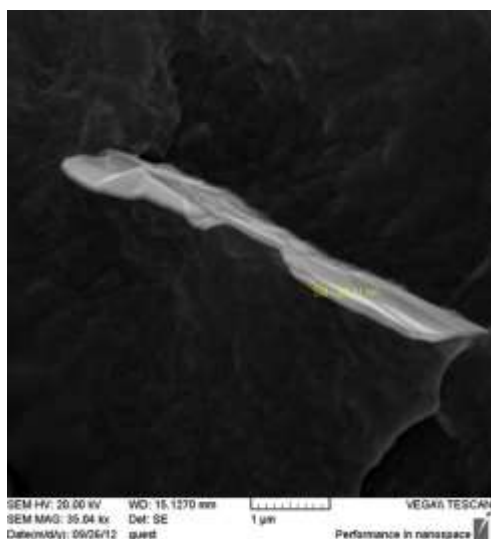
Figure 2: Scanning electron micrograph of 1% graphene in PVDF
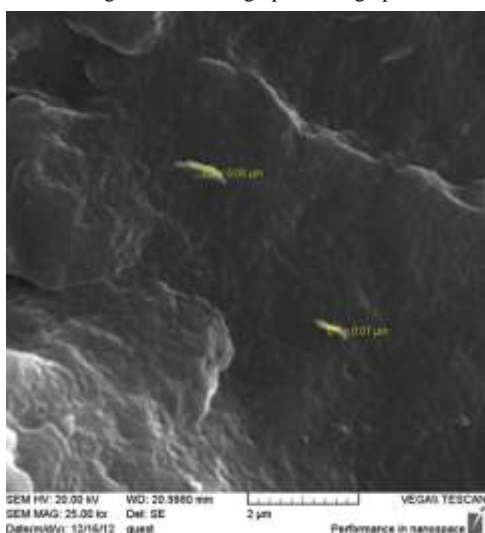
Figure 3: Scanning electron micrograph of 0.5%Cloisite 30B in PVDF
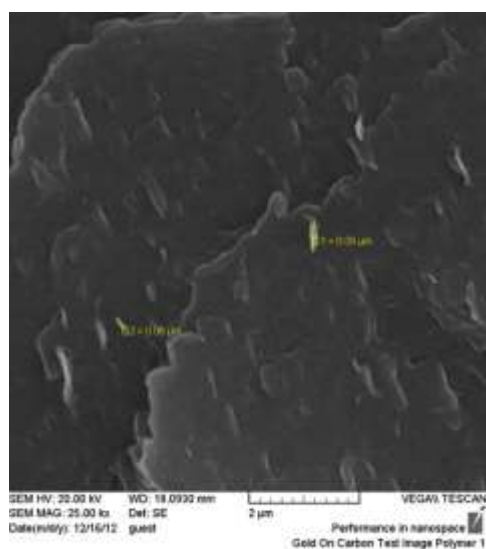
Figure 4: Scanning electron micrograph of 1%Cloisite 30B in PVDF.

In Figure 5 Fourier transform infrared spectra of pure PVDF and its nanocompsites are presented. As seen in the figure, the major peaks are appeared at the same positions in all spectra (alpha crystal's peak at 763 cm^{-1} and beta crystal's peak at 840cm^{-1}). Due to different film thicknesses height of the peaks is changed. Of course, some differences in low frequency region are observable. This is not abnormal due to addition of different materials in PVDF. The height of peaks at 763 and 840cm^{-1} are the interested parameters. Using Equation 1 the content of beta crystals for different nanocomposites was calculated and reported the results in Table 1. According to the data provided in Table 1, incorporation of graphene nanosheets in PVDF results in 6% decrease in beta crystals of polymer as compared with that of pure PVDF. Augmentation of graphene content worsens the situation with 9% decrease in beta crystals. This can be concluded that graphene not only decreases beta crystal content but also show no favorable surface pattern towards beta crystals. An advantage of melt mixing of nanocomposites is that the pure effect of the reinforcements on the crystal structure of PVDF. The case of nanoclay nanocomposites is very different (Table 1). As seen in the table, the composite with 0.5wt% Cloisite 30B results in 6.5% increase in beta crystals. Meanwhile, increasing nanoclay content to 1wt% leads to 4.5% increase in beta crystal content which is almost 2% less than that of 0.5% nanocomposite. This is an important indication of nanoclay surface fitness to promote beta crystal formation. This observation is in full agreement with findings of other researches [45]. The major difference between Cloisite 30B and

graphene surfaces remains in the existence of polar hydroxyl (-OH) groups on the surface of Cloisite 30B and polar organic modifier (quaternary alkyl ammonium salt).

To further investigate the crystal WXRD diffraction patterns are in Figures 6 and 7. As seen in Figure 6, no meaningful difference is observable between patterns of pure PVDF and those of graphene nanocomposites. The large peak at $2\square=25$ belongs to crystalline structure of graphite which is formed by graphene layers. However, a controversial behavior is observed in Figure 7 for Cloisite 30B nanocomposites.

Table 1. Beta crystal content (F($\square$)) of PVDF and its nanocomposites

	Peak height at 763cm⁻¹	Peak height at 840cm⁻¹	F($\square$)
PVDF	0.69534	0.88436	0.50
0.50%Graphene	0.47871	0.47774	0.44
1%Graphene	0.89221	0.78542	0.41
0.5%Clay	0.5343	0.87557	0.56
1%Clay	0.51438	0.7774	0.54
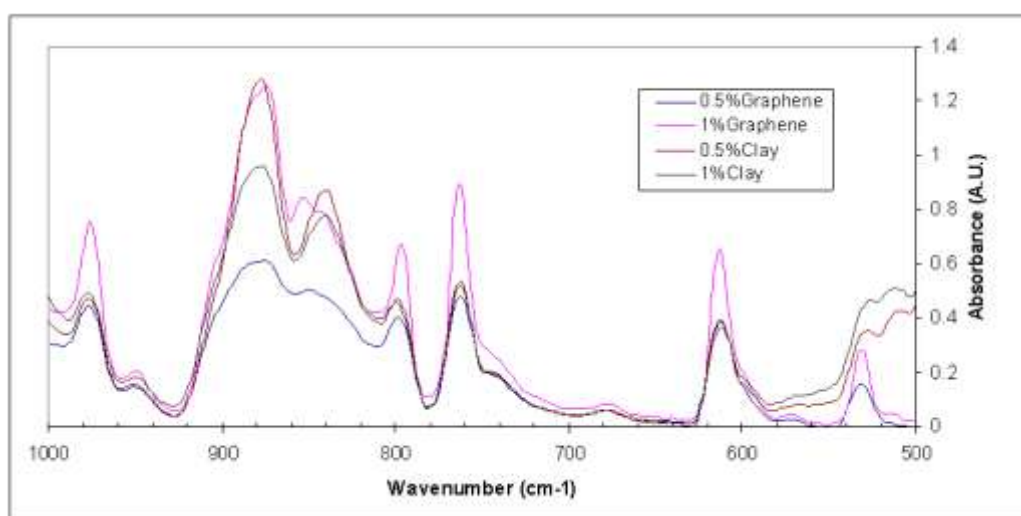
Figure 5. FT-IR spectra of PVDF nanocomposites.
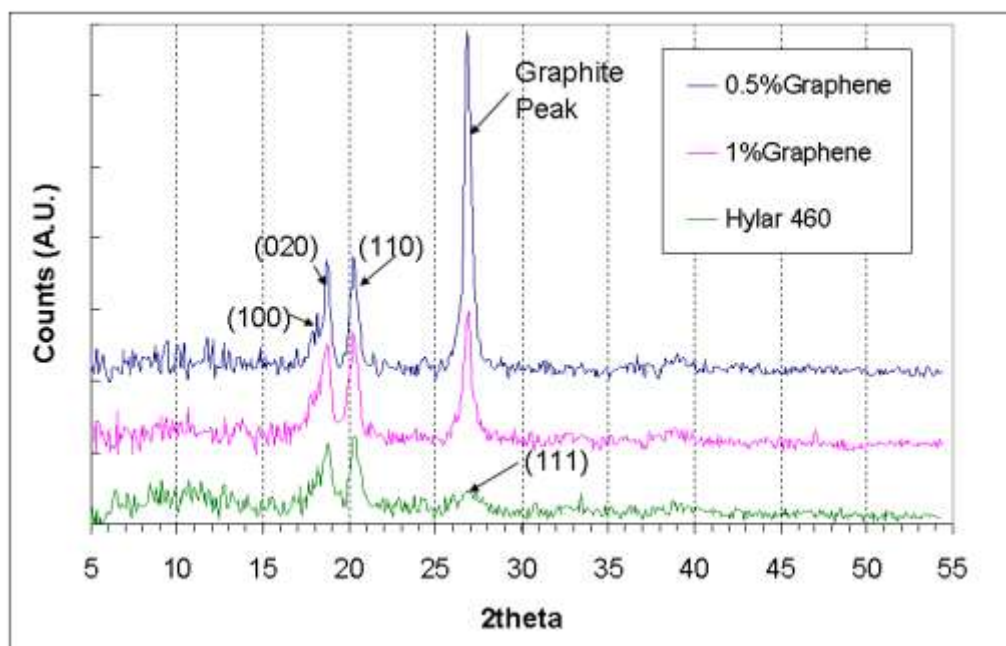
Figure 6: WXRD pattern of graphene-PVDF nanocomposites.
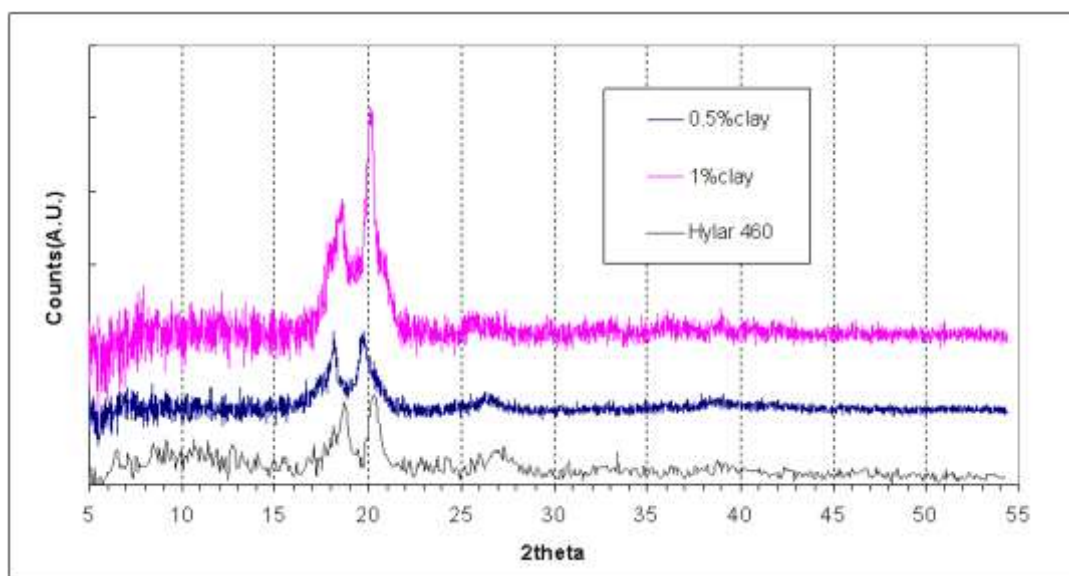
Figure 7. WXRD pattern of nanoclay-PVDF nanocomposites

3.3.Polymer nano-particle interactions

Regarding the morphology and crystalline structure of both clay and graphene modified composites it is evident that the surface properties of these two nanopellets are totally different. Any surface could be characterized by geometrical and energetic parameters. Based on the literature the surface patterns of graphene and Cloisite 30B are very different [30, 46]. Even if these patterns were the same, the energetic aspects of these two nanosheets are very different. These naonosheets are different in surface free energy and surface tension. These parameters of the same dimensions and are provided in Tables 2 and 3 for PVDF, Cloisite30B and graphene. As seen in Table 2 the surface free energy is composed from two components (distributive and polar componenets). Based on Table 2 the surface free energy of Cloisite 30B is very closer to that of PVDF.

Table 2. Surface free energy of nanosheets and PVDF

	Temp. (ºC)	Total Surface free energy (mJ/m2)	Dispersive compone nt (mJ/m2)	Polar compone nt (mJ/m2)	d/dT mJ/m2 K
Cloisite 30B	RT [46] 20 [47] 240 [48]	41.84 35 36	34.7 22.4 23	7.57 12.6 13	0.1
Graphene (fresh)	RT [49]	53 62.2	39.1 47.8	13.9 14.4	-
PVDF	240 [48]	30.3	23.3	7	0

The distributive component of surface free energy of Cloisite 30B is almost coincided on that of PVDF, whereas its polar component nanoclay and graphene are close together and are twice that of PVDF. The surface tension of these three materials are listed in Table 3.

Table 3. Surface tension of naosheets and PVDF

	Temp(ºC)	Surface tension (mN/m)	Dispersive component (mN/m)	Polar component (mN/m)
Cloisite 30B	200[50]	34	23	11
Graphene	190 [51]	52.6	47.7	4.9
PVDF	190 [51]	38	32.6	5.4

As seen, the surface tension of Cloisite 30B is very close to that of PVDF. These groups of data are based on similar measurements therefore, they follow the same trends. Another surface property which controls the state of dispersion any mixture is the interfacial tension existing between two phases of that mixture. In Table 4 the interfacial tension acting in PVDF-Cloisite 30B and PVDF-Graphene systems.

Table 4. Interfacial tension of PVDF-nanosheet systems

	Temp (ºC)		
PVDF-Cloisite 30B [48]	240	HmE	1.8
		GmE	0.9
PVDF-Graphene [51]	190	HmE	2.90
		GmE	1.45

The interfacial tension (energy) of a biphasic system can be calculated using geometric mean equation (GmE, Equation 2, suitable for polar systems) and harmonic mean equation (HmE, Equation 3) of surface tensions of the components [49]:

$$\gamma_{12} = \gamma_1 + \gamma_2 - 2\left(\sqrt{\gamma_1^d \gamma_2^d} + \sqrt{\gamma_1^p \gamma_2^p}\right) \qquad \text{Eq. 2}$$

$$\gamma_{12} = \gamma_1 + \gamma_2 - 4\left(\frac{\gamma_1^d \gamma_2^d}{\gamma_1^d + \gamma_2^d} + \frac{\gamma_1^p \gamma_2^p}{\gamma_1^p + \gamma_2^p}\right) \qquad \text{Eq. 3}$$

where γ_{12}, γ_1, γ_2 stand for interfacial tension and phase 1 and 2 surface tensions and d and p stand for the dispersive and polar components of surface tensions, respectively. According to data enlisted in Table 4 both equations predict lower interfacial tension components for PVDF-Cloisite 30B system. This is in full agreement with finding of this paper. A lower interfacial tension will result in smaller dispersed particles in polymer matrix.

4.Conclusions

Both nanoclay and graphene nanosheets are used to improve piezoelectric properties and crystalline structure of PVDF. Differences in the crystalline structure of PVDF in the presence of these two similar geometry nanosheets are to be investigated. Under the same melt mixing conditions and at the same particle concentration nanoclay (Cloisite 30B) is more effectively dispersed in PVDF matrix. Incorporation of Cloisite 30B increases all-trans conformation (beta-form) in PVDF crystals, whereas addition of graphene leads to a reduction in PVDF beta crystals as compared with that of pure PVDF. Both FT-IR and WXRD techniques confirmed these changes. Two major factors are proposed to differentiate the effects of nanosheets on PVDF crystalline structure, i.e. surface texture and surface free energy (tension).

Comparison of available data showed that the difference of surface free energy and surface tension of PVDF-Cloisite 30B is very lower than those of PVDF-graphene system. Correspondingly, the interfacial tension of PVDF-Cloisite 30B is lower than that of PVDF-graphene system. This reasoning accounts for the observed differences in morphology nanocomposite and crystalline structure of PVDF.

References

[1] Wang TT, Herbert JM, Glass AM (1988) *The Applications of Ferroelectric Polymers*, Chap. 3 and 4, Blakie and Son, New York.
[2] Salimi A, Yousefi AA (2003) FTIR studies of □-phase crystal formation in stretched PVDF films, *Polym. Test.*, 22:699-704.
[3] Bohlén M, Bolton K (2015) Inducing the β-phase of poly(vinylidene fluoride) – a review, Nanosci Nanotech, 1:150110.

[4] Salimi A, Yousefi AA (2004) Conformational changes and phase transformation mechanisms in PVDF solution-cast films, J Polym Sci: Part B:Polym Phys 43:3478-3495.

[5] Yousefi AA (2011) Influence of polymer blending on the crystalline structure of poly(vinylidene fluoride), *Iran. Polym. J.*, 20:109-121.

[6] Yousefi AA (2011) Hybrid poly(vinylidene fluoride)/nanoclay/MWCNT nanocomposites: PVDF crystalline transformation, *Iran.Polym. J.*, 20:725-733.

[7] Kim J-W, Cho W-J, Ha C-S (2002) Morphology, crystalline structure, and properties of poly(vinylidene fluoride)/silica hybrid composites, *J. Polym. Sci., Part B: Polym. Phys*., 40:19-30.

[8] Priya L, Jog JP (2002) Poly(vinylidene fluoride)/clay nanocomposites prepared by melt intercalation: Crystallization and dynamic mechanical behavior studies, *J. Polym. Sci., Part B:Polym Phys* 40:1682–1689.

[9] Shah D, Maiti P, Gunn E, Schmidt DF, Jiang DD, BattCA, Giannelis EP (2004) Dramatic enhancements in toughness of poly(vinylidene fluoride) nanocomposites via nanoclay-directed crystal structure and morphology, *Adv. Mater*., 16:1173-1177.

[10] Sadeghi F, Ajji A (2009) Study of crystal structure of poly(vinylidene fluoride/clay) nanocomposite films: Effect of process conditions and clay type, *Polym Eng Sci* 49:200-207.

[11] El Achaby M, Arrakhiz F-F, Vaudreuil S, Essassi E-M, Qaiss A, Bousmina M (2013) Nanocomposite films of poly(vinylidene fluoride) filled with polyvinylpyrrolidone-coated multiwalled carbon nanotubes: Enhancement of *b*-polymorph formation and tensile properties, Polym. Eng. Sci. 53:34-43

[12] Almazrouei A, Susantyoko RA, Wu CH, Mustafa I, Alhammadi A, Almheiri S (2019) Robust surface-engineered tape-cast and extrusion methods to fabricate electrically-conductive poly(vinylidene fluoride)/carbon nanotube filaments for corrosion-resistant 3D printing applications, Scientific Reports 9:9618

[13] Ansari S, Giannelis EP (2009) Functionalized graphene sheet—poly(vinylidene fluoride) conductive nanocomposites, J Polym Sci: Part B: Polym Phys, 47:888–897

[14] Jiang ZY, Zheng GP, Zhan K, Han Zand Yang J H (2015) Formation of piezoelectric -phase crystallites in poly(vinylidene fluoride)-graphene oxide nanocomposites under uniaxial tensions, J. Phys. D: Appl. Phys. 48:245303

[15] Abbasipour M, Khajavi R. Yousefi AA, Yazdanshenas ME, Razaghian F, Akbarzadeh A (2019) Improving piezoelectric and pyroelectric properties of electrospun PVDF nanofibers using nanofillers for energy harvesting application, Polym Adv Technol 30:279–291

[16] Samadi A, Ahmadi R, Hosseini SM (2019), Influence of TiO$_2$-Fe$_3$O$_4$-MWCNT hybrid nanotubes on piezoelectric and electromagnetic wave absorption properties of electrospun PVDF nanocomposites, Organic Electronics 75:105405

[17] Priya L, Jog JP (2003) Polymorphism in intercalated poly(vinylidene fluoride)/clay nanocomposites, *J. Appl. Polym.Sci*., 89:2036–2040

[18] Priya L, Jog JP (2003), Intercalated poly(vinylidene fluoride)/clay nanocomposites: Structure and properties, *J. Polym. Sci., PartB: Polym. Phys*., 41:31–38

[19] Pramoda KP, Mohamed A, Phang IY, Liu T (2005) Crystal transformation and thermomechanical properties of poly(vinylidenefluoride)/clay nanocomposites, *Polym. Int*., 54:226–232

[20] Pallathadka PK, Tay SS, Tianxi L,Sprenger P (2006) Solid state[19]F-NMR study of crystal transformation in PVDF and its nanocomposites, *Polym. Eng. Sci*., 46:1684–1690.

[21] Dillon DR, Tenneti KK, Li ChY, Ko FK, Sics I, Hsiao BS (2006) On the structure and morphology of poly(vinylidene fluoride)–nanoclay nanocomposites, *Polymer*, 47:1678-1688.

[22] Yu W, Zhao Z, Zheng W, Song Y, Li B, Long B, JiangQ (2008) Structural Characteristics of Poly(vinylidene fluoride)/ClayNanocomposites, *Mater. Lett*., 62:747-750.

[23] Patro TU, Mhalgi MV, Khakhar DV, Misra A (2008) Studieson poly(vinylidene fluoride)–clay nanocomposites: Effect of different clay modifiers, *Polymer*, 49:3486–3499.

[24] Yu L, Cebe P (2009) Effect of nanoclay on relaxation of poly(vinylidene fluoride) nanocomposites, *J. Polym. Sci., PartB: Polym. Phys*. 47:2520–2532.

[25] Yousefi AA, Salarian MM (2012) Effect of polyamide 6 on crystalline structure of polymer in PVDF-nanoclay nanocomposite, Iran J PolymSci Tech 25:41-51.

[26] Bodkhe S, Rajesh PSM, Kamle S, Verma V (2014) Beta-phase enhancement in polyvinylidene fluoride through filler addition: comparing cellulose with carbon nanotubes and clay, J Polym Res 21:434-445

[27] Roopa TS, Narasimhamurthy HN, Swathi HS, Angadi G, Harish DVN (2019) Synthesis and characterization of spin-coated clay/PVDF thin films, *Bull. Mater. Sci.* 42:15 (8 pages)

[28] Schiefferdecker VM, Barra GMO, Ramôa SDA, Merlini C (2019) Comparative study of the structure and properties of poly(vinylidene fluoride)/montmorillonite-polypyrrole nanocomposites prepared by electrospinning and solution casting frontiers in materials, 6: Article 193 (12 pages)

[29] Choi W, Lee J-W (2012) Graphene Synthesis and Applications, CRC Press, Tailor & Francis Group, New York

[30] Mishra S, Hansora Dh (2018) Graphene Nanomaterials: Fabrication, Properties and Applications, Pan Stanford Publication Pte. Ltd., Taylor & Francis, USA

[31] Ansari S, Giannelis EP (2009) Functionalized graphene sheet—poly(vinylidene fluoride) conductive nanocomposites, J PolymPhys Part B: PolymPhys 47: 888–897.

[32] El Achaby M, Arrakhiz FZ, Vaudreuil S, Essassi EM, Qaiss A (2012) Piezoelectric-polymorph formation and properties enhancement in graphene oxide–PVDF nanocomposite films, Appl Surf Sci 258:7668– 677.

[33] El Achaby M, Arrakhiz FZ, Vaudreuil S, Essassi EM, Qaiss A, Bousmina M (2013) Preparation and characterization of melt-blended graphene nanosheets–poly(vinylidene fluoride) nanocomposites with enhanced properties, J. Appl. Polym. Sci. 127:4697–4707.

[34] Ataur Rahman Md, Chung G-S (2013) Synthesis of PVDF-graphene nanocomposites and their properties, J Alloys Compounds, doi:10.1016/j.jallcom.2013.07.118

[35] Jang JW, Min BG, Yeum JH, JeongYG (2013) Structures and physical properties of graphene/PVDF nanocomposite films prepared by solution-mixing and melt-compression, Fibers and Polymers 14:1332-1338.

[36] Liu F, Huo R, Huang X, Jiang P (2013) Effect of Processing Method on the Dielectric Behavior of Graphene Oxide/PVDF Nanocomposites, IEEE International Conference on Solid Dielectrics, Bologna, Italy, June 30–July 4.

[37] Mohamadi S, Sharifi-Sanjani N, and Foyouhi A (2013) Evaluation of graphene nanosheets influence on the physical properties of PVDF/PMMA blend, J Polym Res 20:46

[38] Huang L, Lu C, Wang F, Wang L (2014) Preparation of PVDF/graphene ferroelectric composite films by in situ reduction with hydrobromic acids and their properties, RSC Adv., 4:45220

[39] Wang B, Gong X, Li J, Shang Y, Shi D, Christiansen JC, Yu D, Jiang S (2015) Double equilibrium melting temperatures and zero growth temperature of PVDF in PVDF/graphene composites, J Polym Res 22:244

[40] An N, Liu S, Fang C, Yu R, Zhou X, Cheng Y (2015) Preparation and Properties of □-Phase Graphene Oxide/PVDF Composite Films, J. Appl. Polym. Sci. 132: 41577

[41] Thakre A, Borkar H, B.P Singh BP, Kumar A (2015) Electroforming free high resistance resistive switching of graphene oxide modified polar-PVDF, *RSC Adv.*, DOI: 10.1039/C5RA08663A

[42] Jiang Z Y, Zheng G P, Zhan K, Han Z, Yang J H (2015) Formation of piezoelectric β-phase crystallites in poly(vinylidene fluoride)-graphene oxide nanocomposites under uniaxial tensions, J. Phys. D: Appl. Phys. 48:245303

[43] Zheng GP, Jiang ZY, Han Z, Yang JH (2016) Mechanical and electro-mechanical properties of three-dimensional nanoporous graphene-poly(vinylidene fluoride) composites, eXPRESS Polymer Letters 10:730–741.

[44] Fortunato M, Bidsorkhi HC, De Bellis G, Sarto F, Sarto MS (2017) Piezoelectric response of graphene-filled PVDF nanocomposites through piezoresponse force microscopy (PFM), Proceedings of the 17th IEEE International Conference on Nanotechnology Pittsburgh, USA, July 25-28.

[45] Abbasipour M, Khajavi R. Yousefi AA, Yazdanshenas ME, Razaghian F, Akbarzadeh A (2017), The piezoelectric response of electrospun PVDF nanofibers with graphene oxide, graphene, and halloysite nanofillers: a comparative study, J Mater Sci: Mater Electron 28:15942-15952

[46] Jawaid M, Qaiss A-K, Bouhfid R, Eds (2016) Nanoclay Reinforced Polymer Composites: Natural Fibre/Nanoclay Hybrid Composites, Springer Nature.

[47] Ianchis R, Corobea MC, Donescu D, Rosca ID, Cinteza LO, Nistor LC, Vasile E, Marin A, Preda S (2012) Advanced functionalization of organoclay nanoparticles by silylation and their polystyrene nanocomposites obtained by miniemulsion polymerization, J Nanopart Res 14:1233, doi:10.1007/s11051-012-1233-6

[48] Entezam M, Khonakdar HA, Yousefi AA, Jafari SH, Wagenknecht U, Heinrich G (2013) Dynamic and transient shear start-up flow experiments for analyzing nanoclay localization in PP/PET blends: Correlation with microstructure, Macromol Mater Eng 298:113–126.

[49] Lin H-M, Behera K, Yadav M and Chiu F-Ch (2020) Polyamide 6/poly(vinylidene fluoride) blend-based nanocomposites with enhanced rigidity: Selective localization of carbon nanotube and organoclay, Polymers 12:184; doi:10.3390/polym12010184

[50] Kozbial A, Li Zh, Conaway C, McGinley R, Dhingra Sh, Vahdat V, Zhou F, D'Urso B, Liu H, Li L (2014) Study on the surface energy of graphene by contact angle measurements, Langmuir 30:8598−8606.

[51] Razavi Aghjeh M, Kazerouni Y, Otadi M, Khonakdar H A, Jafari S H, Ebadi-Dehaghani H, Mousavi S (2018) A combined experimental and theoretical approach to quantitative assessment of microstructure in PLA/PP/organo-clay nanocomposites; wide-angle x-ray scattering and rheological analysis, Composites Part B 137:235–246.

[52] Behera K, Yadav M, Chiu F-C, Rhee K Y (2019) Graphene nanoplatelet-reinforced poly(vinylidene fluoride)/high density polyethylene blend-based nanocomposites with enhanced thermal and electrical properties, Nanomaterials 9:361; doi:10.3390/nano9030361